Anal. Chem. **1996**, *68*, 2676–2685

Two-Dimensional Model of a Direct Current Glow Discharge: Description of the Argon Metastable Atoms, Sputtered Atoms, and Ions

A. Bogaerts* and R. Gijbels

Department of Chemistry, University of Antwerp (UIA), Universiteitsplein 1, B-2610 Wilrijk-Antwerp, Belgium

A two-dimensional model is presented that describes the behavior of argon metastable atoms, copper atoms, and copper ions in an argon direct current glow discharge, in the standard cell of the VG9000 glow discharge mass spectrometer for analyzing flat samples. The model is combined with a previously developed model for the electrons, argon ions, and atoms in the same cell to obtain an overall picture of the glow discharge. The results of the present model comprise the number densities of the described plasma species, the relative contributions of different production and loss processes for the argon metastable atoms, the thermalization profile of the sputtered copper atoms, the relative importance of the different ionization mechanisms for the copper atoms, the ionization degree of copper, the copper ion-to-argon ion density ratio, and the relative roles of copper ions, argon ions, and atoms in the sputtering process. All these quantities are calculated for a range of voltages and pressures. Moreover, since the sticking coefficient of copper atoms on solid surfaces is not well-known in the literature, the influence of this parameter on the results is briefly discussed.

Glow discharges are becoming widely accepted as sources for analytical techniques, like mass spectrometry, optical emission spectrometry, and atomic absorption spectrometry.[1,2] To acquire better results in these fields of application, a good understanding of the glow discharge is desirable. One way to attempt this is by mathematical modeling. In a previous paper,[3] a two-dimensional model was developed to describe the electrons, argon ions, and fast argon atoms in a direct current (dc) glow discharge. These species are of major importance for the description of the electrical characteristics of the glow discharge. However, besides the electrons, argon ions, and argon atoms, other kinds of species are present in the glow discharge plasma as well. The cathode of the glow discharge consists of the material to be analyzed. Upon bombardment of the cathode surface by the plasma species, atoms of the cathode material are released and enter the plasma. Since these atoms are of special interest for analytical purposes, the present model focuses on these species. The model is intended to describe a glow discharge used as an ion source for mass spectrometry. Therefore, the behavior of the atoms of the cathode material is calculated, as well as the behavior of the corresponding ions. Ionization processes incorporated in the model are Penning ionization by argon metastable atoms (eq 1), asymmetric charge transfer by argon ions (eq 2) and electron impact ionization (eq 3). The data required to calculate the latter two processes (i.e., the argon ion density and electron flux) are taken from the model described in ref 3. To compute the Penning ionization process, the argon metastable atom density is required, which will therefore also be calculated in this paper. Hence, the present model treats the argon metastable atoms, the sputtered atoms and the corresponding ions.

$$Cu^0 + Ar^*_m \rightarrow Cu^+ + Ar^0 + e^- \quad (1)$$

$$Cu^0 + Ar^+ \rightarrow Cu^+ + Ar^0 \quad (2)$$

$$Cu^0 + e^- \rightarrow Cu^+ + 2e^- \quad (3)$$

The behavior of the argon metastable atoms is calculated with a balance equation taking into account all known production and loss processes. The sputtered atoms and corresponding ions are described with three combined models, i.e., (i) a Monte Carlo model to compute the thermalization of the sputtered atoms after they leave the cathode, (ii) a fluid model to describe the transport of the atoms and ions, and (iii) a Monte Carlo model to simulate the behavior of the ions explicitly in the cathode dark space. Copper is taken as an example, but the calculations can be carried out for other elements, too.

The models have previously been presented in one dimension, except for the model describing the thermalization of the sputtered atoms, which was previously developed in three dimensions;[4] i.e., the one-dimensional model of the metastable atoms was developed in ref 5, and the one-dimensional model describing the sputtered atoms and ions was dealt with in ref 6. In the present paper, the models are extended to the complete three-dimensional geometry, corresponding to a standard cell of the VG9000 glow discharge mass spectrometer (VG Elemental, Fisons). By coupling the present model with the two-dimensional model described in ref 3, an overall picture of the most important species in the dc glow discharge in argon can be obtained.

DESCRIPTION OF THE MODEL

A. Model Assumptions. As in ref 3, the discharge geometry to which the models are applied is that of the so-called new

(1) Harrison, W. W. In *Glow Discharge Mass Spectrometry*, in *Inorganic Mass Spectrometry*; Adams, F., Gijbels, R., Van Grieken, R., Eds.; Wiley: New York, 1988; Chapter 3.
(2) Marcus, R. K. *Glow Discharge Spectroscopies*; Plenum Press: New York, 1993.
(3) Bogaerts, A.; Gijbels, R.; Goedheer, W. J. *Anal. Chem.* **1996**, *68*, 2296–2303.
(4) Bogaerts, A.; van Straaten, M.; Gijbels, R. *J. Appl. Phys.* **1995**, *77*, 1868–1874.
(5) Bogaerts, A.; Gijbels, R. *Phys. Rev. A* **1995**, *52*, 3743–3751.
(6) Bogaerts, A.; Gijbels, R. *J. Appl. Phys.* **1996**, *79*, 1279–1286.

S0003-2700(95)01206-6 CCC: $12.00

standard discharge cell of the VG9000 glow discharge mass spectrometer (VG Elemental, Fisons) for analyzing flat samples, with argon as the discharge gas and copper as the cathode (see Figure 1 of ref 3). Since the glow discharge cell is cylindrically symmetrical, the three-dimensional geometry can be reduced to two dimensions, and the model is therefore actually a two-dimensional one. It is again assumed that the cell is in a closed configuration, without gas inlet or exit slit to the mass spectrometer, which implies that there is no gas flow and that the argon gas is more or less at rest, uniformly distributed throughout the cell. This approximation seems to be justified, since the gas consumption rate in the glow discharge cell is, indeed, very low (1 gas tank (70 bar) in 5 years). Moreover, the gas inlet area is 0.0013 cm^2 (0.4 mm diameter), and the exit slit area is 0.001 cm^2 (1 mm long and 0.1 mm wide). Both areas are small for a cell volume of about 4.9 cm^3, and so it is expected that the gas inlet and exit slit will have no large effect on the calculations. This follows also from experimental observations. Indeed, the gas inlet is at the side walls and would therefore perturb the cylindrical symmetry of the cell. Nevertheless, the experimentally obtained crater profiles are found to be cylindrically symmetrical.

The plasma is assumed to consist of the following species: argon gas atoms at rest (Ar^0), singly charged positive argon ions (Ar^+), fast argon atoms (Ar^0_f), fast and slow electrons, argon metastable atoms (Ar^*_m), and atoms and ions of the cathode material (i.e., Cu^0 and Cu^+). The argon ions, fast argon atoms, and fast and slow electrons were described in the model of ref 3. The present model treats the argon metastable atoms and the copper atoms and ions.

B. Argon Metastable Atom Model. The density of the metastable atoms is calculated by solving a balance equation composed of the different production and loss processes of the metastable atoms. Argon possesses two metastable levels, lying close to each other, i.e., the ($3p^54s$) $^3P_2$ level and the ($3p^54s$) $^3P_0$ level, at 11.55 and 11.72 eV above the ground state, respectively. Since the $^3P_0$ level is a factor of 5−10 less populated than the $^3P_2$ level,[7,8] and since we are interested only in the total argon metastable atom density, the two metastable levels are combined in one collective level, lying at 11.55 eV.

The production processes incorporated in the model are (i) fast electron impact excitation from ground state argon atoms, including cascading from higher energy levels, (ii) fast argon ion impact excitation from ground state argon atoms, (iii) fast argon atom impact excitation from ground state argon atoms, and (iv) radiative recombination between argon ions and slow electrons. Loss processes taken into account comprise (i) fast electron impact ionization from the metastable level, (ii) fast electron impact excitation from the metastable level to higher energy levels, (iii) electron quenching, which means collision with thermalized electrons, leading to the transfer of the metastable level to the nearby resonant levels (i.e., the ($3p^54s$) $^3P_1$ and the ($3p^54s$) $^1P_1$ levels, at 11.62 and 11.83 eV above the ground state, respectively), (iv) metastable atom−metastable atom collisions resulting in the ionization of one of the atoms, (v) Penning ionization of the sputtered copper atoms, (vi) two-body collisions with argon ground state atoms, and (vii) three-body collisions with argon ground state atoms. An additional loss process results from diffusion to the walls, followed by deexcitation at the walls. Since the gas is assumed to be pure argon, destruction of argon metastable atoms by impurity gas molecules is neglected. These production and loss processes yield the following two-dimensional balance equation:

$$\frac{\partial n_{Ar^*_m}}{\partial t} - D_{Ar^*_m}\frac{1}{r}\frac{\partial}{\partial r}\left(r\frac{\partial n_{Ar^*_m}}{\partial r}\right) - D_{Ar^*_m}\frac{\partial^2 n_{Ar^*_m}}{\partial z^2} = R_{prod}(z,r) - R_{loss}(z,r) \quad (4)$$

where

$$R_{prod}(z,r) = R_{e,exc}(z,r) + R_{i,exc}(z,r) + R_{a,exc}(z,r) + k_{recomb}n_{e,s}(z,r)n_{Ar^+}(z,r) \quad (5)$$

$$R_{loss}(z,r) = R_{ion,met}(z,r) + R_{exc,met}(z,r) + k_{quen}n_{e,s}(z,r)n_{Ar^*_m}(z,r) + 2k_{met}[n_{Ar^*_m}(z,r)]^2 + k_{Pi}n_{Cu}(z,r)n_{Ar^*_m}(z,r) + k_{2B}n_{Ar^0}(z,r)n_{Ar^*_m}(z,r) + k_{3B}[n_{Ar^0}(z,r)]^2 n_{Ar^*_m}(z,r)$$

The first term in eq 4 is zero under the present steady state conditions. R represents the rate of a process, and k means the rate constant; z and r are the axial and radial coordinates, respectively; n represents the density; and D is the diffusion coefficient. The fourth term on the right-hand side of the equation involving R_{loss}, i.e., the term describing the loss by argon metastable atom−metastable atom collisions, contains a factor 2. Indeed, two metastable argon atoms are lost in one such collision process. A more exhaustive treatment and numerical values of the different coefficients can be found in ref 5.

The loss due to diffusion and subsequent deexcitation at the walls is determined by the boundary conditions, i.e., $n_{Ar^*_m} = 0$ at all walls. The balance equation (differential equation) is converted into a finite difference equation and then solved with the Thomas algorithm.[9]

C. Model of the Copper Atoms and Ions. *(1) Description of the Thermalization Process of Copper Atoms by a Monte Carlo Method.* The atoms of the cathode material (copper) are sputtered away from the cathode due to the bombardment by plasma species (i.e., argon ions, fast argon atoms, and copper ions). They arrive in the plasma and lose their initial energies of a few electronvolts almost immediately upon collisions with the argon gas particles, whereafter they diffuse further into the plasma or back toward the cathode. Since the thermalization process is much faster than the diffusion, it can be assumed to be already finished when diffusion starts.[10] Both processes can therefore be separated in time when modeling the behavior of the sputtered atoms, i.e., the simulation of the thermalization process results in a thermalization profile, which is used afterward as the starting distribution in the description of the diffusion process (see further discussion).

The thermalization process is described by a three-dimensional Monte Carlo simulation, i.e., calculating the trajectory of the sputtered atoms by Newton's laws and treating the elastic

(7) Tachibana, K. *Phys. Rev. A* **1986**, *34*, 1007−1015.
(8) Kolts, J. H.; Setser, D. W. *J. Chem. Phys.* **1978**, *68*, 4848−4859.
(9) von Rosenberg, D. U. *Methods for the Numerical Solution of Partial Differential Equations*; Elsevier: New York, 1969.
(10) Valles-Abarca, J. A.; Gras-Marti, A. *J. Appl. Phys.* **1984**, *55*, 1370−1378.

collisions with argon gas atoms by random numbers. The complete description of this model is given in ref 4.

(2) Description of the Further Transport of Copper Atoms and Ions by a Fluid Model. When the copper atoms have been thermalized, further transport is diffusion dominated. The production term of copper atoms is therefore given by the flux of sputtered copper atoms from the cathode, J_0, multiplied by the normalized spatial distribution of the copper atoms after thermalization, i.e., the thermalization profile, $F_T(z,r)$. The copper atoms can be ionized in the glow discharge plasma, leading to the formation of copper ions. The three ionization mechanisms incorporated in the model are Penning ionization by argon metastable atoms ($k_{PI}n_{Ar^+_m}$), asymmetric charge transfer by argon ions ($k_{CT}n_{Ar^+}$), and electron impact ionization ($R_{EI,Cu}$). These processes determine the loss of copper atoms and, at the same time, the production of copper ions ($R_{loss,Cu^0} = R_{prod,Cu^+}$). The transport of the copper ions is controlled by diffusion and by migration in the electric field. Loss of copper ions by electron–ion recombination, is neglected.[11] The above-described behavior of copper atoms and ions is expressed by the following equations:

$$\frac{\partial n_{Cu}}{\partial t} - D_{Cu}\frac{1}{r}\frac{\partial}{\partial r}\left(r\frac{\partial n_{Cu}}{\partial r}\right) - D_{Cu}\frac{\partial^2 n_{Cu}}{\partial z^2} = R_{prod,Cu}(z,r) - R_{loss,Cu}(z,r)$$

$$\frac{\partial n_{Cu^-}}{\partial t} + \mu_{Cu^-}\frac{1}{r}\frac{\partial}{\partial r}(r n_{Cu^-}E_r) - D_{Cu^-}\frac{1}{r}\frac{\partial}{\partial r}\left(r\frac{\partial n_{Cu^-}}{\partial r}\right) + \mu_{Cu^+}\frac{\partial}{\partial z}(n_{Cu^-}E_z) - D_{Cu^-}\frac{\partial^2 n_{Cu^+}}{\partial z^2} = R_{prod,Cu^+}(z,r) \quad (6)$$

$$R_{prod,Cu}(z,r) = J_0 F_T(z,r)$$

$$R_{loss,Cu}(z,r) = R_{prod,Cu^+}(z,r) = n_{Cu}(z,r)[R_{EI,Cu}(z,r) + k_{PI}n_{Ar^+_m}(z,r) + k_{CT}n_{Ar^-}(z,r)]$$

where μ represents the mobility of the ions, and the other symbols are as defined previously. The full explanation and numerical values of the different terms can be found in ref 6. The value of the Penning ionization rate constant is assumed to be 2.36×10^{-10} $cm^3\ s^{-1}$, as in ref 6. The value of the charge transfer rate constant between Ar^+ and Cu^0 is taken to be 2×10^{-10} $cm^3\ s^{-1}$, which is adapted from ref 12; rate constants of this process are very difficult to find in the literature. This process occurs only if the energy difference between the argon ion ground state (or metastable level) and the resulting analyte ion is "sufficiently small". Since the rate constant was not directly measured in ref 12, but was deduced from a fitting procedure in a mathematical model, it can be subject to uncertainties. However, k_{CT} is of the same order of magnitude as k_{PI} when the ion possesses suitable energy levels for asymmetric charge transfer.[13,14] Copper ions possess no energy levels having good overlap with the argon ion ground state level; however, there is one energy level that overlaps well with the argon ion metastable energy level.[15] Since we could not find more accurate data, we used the above-mentioned k_{CT} value in our model.

The above continuity equations of copper ions and atoms are coupled through $R_{loss,Cu} = R_{prod,Cu^+}$. The coupled equations are converted into finite difference equations, and the resulting bi-tridiagonal system is solved with the extended Thomas algorithm.[9]

The boundary conditions for these equations are somewhat different from the ones used in ref 6. For the copper ions, the boundary conditions of $n_{Cu^+} = 0$ (i.e., sticking coefficient $A_+ = 1$) and $\nabla n_{Cu^+} = 0$ (i.e., sticking coefficient $A_+ = 0$) at all walls gave exactly the same results, which tells us that the boundary conditions have no significant influence for Cu^+. This was also observed by van Veldhuizen and de Hoog.[11] For the copper atoms, however, varying the boundary conditions between $n_{Cu} = 0$ (sticking coefficient $A_0 = 1$) and $\nabla n_{Cu} = 0$ (sticking coefficient $A_0 = 0$) yielded different results for the copper atom density. A lot of models describing the behavior of sputtered atoms use the boundary condition $n_M = 0$ without justification.[6,10,16,17] However, it has been suggested that the sticking coefficient of atoms, A_0, is different from 1.[11,18] In ref 11, it is stated that A_0 may vary between 0.5 and 0.01, depending largely on the structure of the surface. We have measured three-dimensional number density profiles of sputtered tantalum atoms in a six-way cross glow discharge with laser-induced fluorescence.[19] These measured density profiles showed good agreement with the modeling calculations if a sticking coefficient of 0.5 was assumed. Therefore, we have adopted this value of 0.5 also in the present model. Since the actual value of A_0 is unknown, we will discuss briefly the influence of this parameter on the results in this paper.

(3) Description of the Behavior of the Copper Ions in the Cathode Dark Space by a Monte Carlo Model. The copper ions are not in hydrodynamic equilibrium in the cathode dark space (CDS), where a strong electric field is present. Indeed, the ions gain more energy from the electric field than they lose due to collisions. In ref 6, it was shown that the calculated flux energy distribution of the copper ions bombarding the cathode is characterized by a peak at maximum energy, i.e., the energy corresponding to the full voltage drop in the CDS. This means that most of the copper ions have lost no appreciable energy due to collisions in the CDS. As was illustrated in ref 6, the calculated energy distribution was in excellent agreement with experimentally measured energy distributions at the cathode of the VG9000 glow discharge mass spectrometer.[20]

Since the copper ions are not in hydrodynamic equilibrium with the strong electric field in the CDS, they are treated not only with a fluid model (see section 2 above) but also explicitly, in the CDS, with a Monte Carlo simulation. Input data for this model are the flux of copper ions entering the CDS from the negative glow (NG) and the number of copper ions created in the CDS. Both data are taken from the above-described fluid approach. Only elastic collisions with argon gas atoms are taken into account in

(11) van Veldhuizen, E. M.; de Hoog, F. J. *J. Phys. D: Appl. Phys.* **1984**, *17*, 953–968.
(12) Rae, S. C.; Tobin, R. C. *J. Appl. Phys.* **1988**, *64*, 1418–1424.
(13) Baltayan, P.; Pebay-Peyroula, J. C.; Sadeghi, N. *J. Phys. B* **1985**, *18*, 3615–3628.
(14) Baltayan, P.; Pebay-Peyroula, J. C.; Sadeghi, N. *J. Phys. B* **1986**, *19*, 2695–2702.
(15) Steers, E. B. M.; Fielding, R. J. *J. Anal. Atom. Spectrom.* **1987**, *2*, 239–244.
(16) van Straaten, M.; Vertes, A.; Gijbels, R. *Spectrochim. Acta, Part B* **1991**, *46*, 283–290.
(17) van Straaten, M.; Gijbels, R.; Vertes, A. *Anal. Chem.* **1992**, *64*, 1855–1863.
(18) Allott, R. M.; Kubinyi, M.; Grofcsik, A.; Jones, W. J.; Mason, R. S. *J. Chem. Soc., Faraday Trans.* **1995**, *91*, 1297–1301.
(19) Bogaerts, A.; Wagner, E.; Smith, B. W.; Winefordner, J. D.; Pollmann, D.; Harrison, W. W.; Gijbels, R. *Spectrochim. Acta Part B*, submitted.
(20) van Straaten, M.; Bogaerts, A.; Gijbels, R. *Spectrochim. Acta Part B* **1995**, *50*, 583–605.

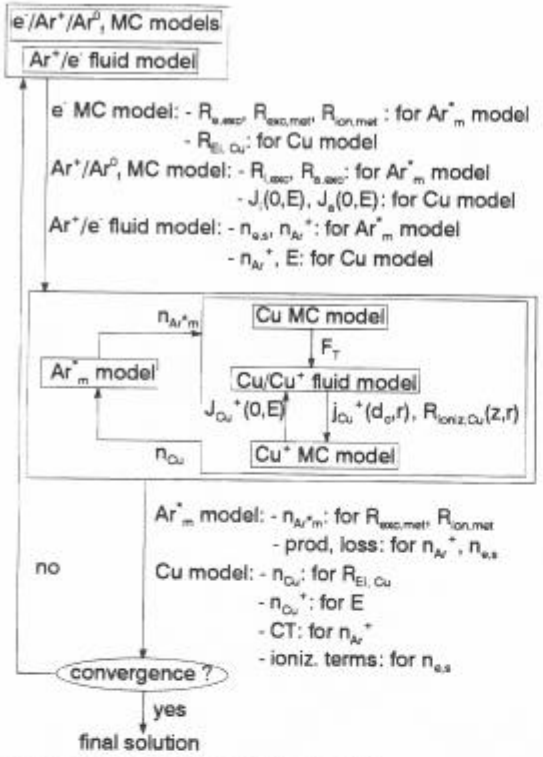

Figure 1. Flow chart of the combined models.

this Monte Carlo model, since the other kinds of collisions are considered to be negligible.[6] The complete description of this model (i.e., calculation of the trajectory by Newton's laws, treatment of the collisions by random numbers, coupling to the copper atom and ion fluid model, etc.) is given in ref 6. One of the important results of this model is the flux energy distribution of the copper ions bombarding the cathode, which is used, together with the flux energy distribution of argon ions and fast argon atoms at the cathode, to calculate the flux of sputtered copper atoms from the cathode, J_0.

D. Combination of the Different Models. The different models described in the present paper and in ref 3 are coupled and solved by an iterative procedure, in order to obtain an overall picture of the glow discharge. The flow chart of the coupling is presented in Figure 1.

The fast electron, argon ion, and fast argon atom Monte Carlo models ($e^-/Ar^+/Ar^0_f$ MC models) and the argon ion–slow electron fluid model (Ar^+/e^- fluid model) are solved iteratively until convergence, similar to the explanation in Figure 3 of ref 3. The details are not included here, since it would make the present flow chart too complicated.

The results of these calculations that are of importance for the argon metastable atom model (Ar^*_m model) and for the copper atom and ion model (Cu model) are the following. The e^- MC model yields the electron impact excitation rate to the metastable level ($R_{e,exc}$) and the electron impact excitation and ionization rates from the metastable level ($R_{exc,met}$ and $R_{ion,met}$), which are used as production and loss terms, respectively, in the Ar^*_m model. It also gives the electron impact ionization rate of copper atoms ($R_{EI,Cu}$), which is used as loss term for Cu and production term for Cu^+ in the Cu model. In the Ar^+/Ar^0_f MC model, one calculates the ion and atom impact excitation rates to the metastable level ($R_{i,exc}$ and $R_{a,exc}$), which are production terms in the Ar^*_m model. Also, the argon ion and atom flux energy distributions at the cathode ($J_i(0,E)$ and $J_a(0,E)$, respectively) are obtained; these values are needed in order to calculate the flux of sputtered copper atoms in the Cu model. Finally, the Ar^+/e^- fluid model yields the argon ion and slow electron number densities (n_{Ar^+} and $n_{e,s}$), which are exploited in some production and loss terms of the Ar^*_m model (i.e., electron–ion recombination and electron quenching, respectively). Moreover, the argon ion number density (n_{Ar^+}) and the electric field distribution (E) resulting from this Ar^+/e^- fluid model are made use of in the Cu model for the charge transfer ionization and for the migration component of the copper ion transport, respectively.

With these input values, the Ar^*_m model and the Cu model are solved. The Ar^*_m model yields the argon metastable atom density ($n_{Ar^*_m}$), which is required for the Penning ionization rate of the copper atoms in the Cu model. Then, the Cu model is calculated. The Monte Carlo model of the copper atom thermalization process (Cu MC model) yields the thermalization profile (F_T), which is the input in the Cu atom–ion fluid model (Cu/Cu^+ fluid model). Results of the Cu/Cu^+ fluid model include, among others, the flux of copper ions entering the CDS ($j_{Cu^+}(d_c,r)$, where d_c represents the (axial) length of the CDS) and the number of copper ions created within the CDS ($R_{ioniz,Cu}(z,r)$), where both are needed in the Cu ion Monte Carlo model (Cu^+ MC model). One of the results of the Cu^+ MC model is the flux energy distribution of copper ions bombarding the cathode ($J_{Cu^+}(0,E)$), which allows the calculation of the updated flux of copper atoms sputtered from the cathode, used in the Cu MC model and in the Cu/Cu^+ fluid model. The Cu MC model, the Cu/Cu^+ fluid model, and the Cu^+ MC model are solved iteratively until convergence is reached (typically after two or three iterations). The resulting copper atom number density (n_{Cu}) is then put into the Ar^*_m model for the Penning ionization loss term. The Ar^*_m model and the total Cu model are solved iteratively until convergence, which is reached typically after two iterations.

The results of the Ar^*_m model and the Cu model that are of importance for the $e^-/Ar^+/Ar^0_f$ MC models and for the Ar^+/e^- fluid model, are the following. The Ar^*_m model yields the argon metastable atom number density ($n_{Ar^*_m}$), which is used to recalculate the electron impact excitation and ionization rates ($R_{exc,met}$ and $R_{ion,met}$) in the e^- MC model. Moreover, some of the production and loss terms can influence the argon ion and slow electron number densities in the Ar^+/e^- fluid model, although this effect is almost negligible. The Cu model yields the copper atom number density (n_{Cu}), which determines the new electron impact ionization rate of copper ($R_{EI,Cu}$) in the e^- MC model. The copper ion number density (n_{Cu^+}) can influence the electric field distribution in the Ar^+/e^- fluid model. The asymmetric charge transfer ionization term can have an effect on the argon ion density (n_{Ar^+}) in the Ar^+/e^- fluid model, and the three ionization terms of copper influence the slow electron number density ($n_{e,s}$) in the Ar^+/e^- fluid model. However, all of these effects are rather small.

These data are again introduced into the $e^-/Ar^+/Ar^0_f$ MC model and in the Ar^+/e^- fluid model, and the entire model is solved until final convergence is reached. For the discharge conditions we investigated, the results of the Ar^*_m model and of the Cu model had almost no effect on the $e^-/Ar^+/Ar^0_f$ model and

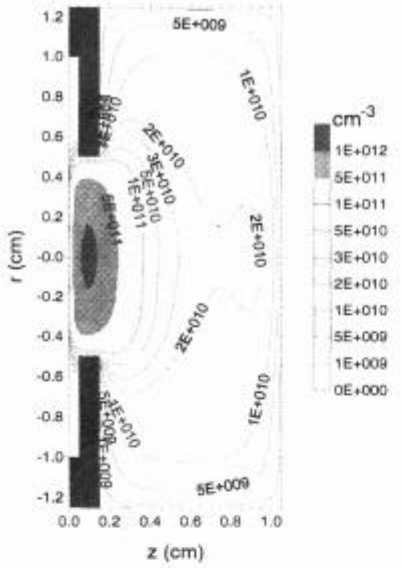

Figure 2. Density profile of the argon metastable atoms at 75 Pa and 1000 V.

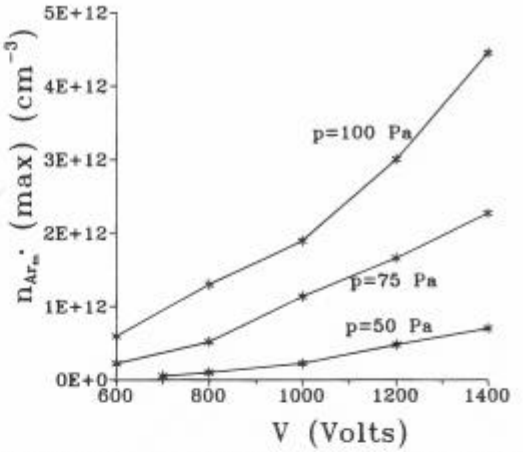

Figure 3. Maximum argon metastable atom density as a function of voltage at three pressures.

the Ar^+/e^- fluid model, so that final convergence is actually reached after just one iteration.

RESULTS AND DISCUSSION

Results will be presented for an argon discharge with a copper cathode in the new VG9000 glow discharge cell to analyze flat samples[21] at discharge conditions of 1000 V and 75 Pa. For a gas temperature of 360 K, the electrical current was then calculated from the argon ion and electron fluxes in ref 3 to be 3.4 mA. The calculated current is hence in reasonable agreement with experimental values, which demonstrates that the model of ref 3 yields realistic results. These voltage, pressure, and current values are typical discharge conditions of the VG9000 glow discharge mass spectrometer. Moreover, the influence of voltage and pressure will be investigated in the voltage range between 600 and 1400 V and in the pressure range of 50−100 Pa (corresponding to calculated electrical currents between 0.4 and 11 mA).

A. Results of the Argon Metastable Atoms. Figure 2 shows the two-dimensional argon metastable atom number density profile at 1000 V and 75 Pa. A pronounced maximum of about 10^{12} cm^{-3} is reached close to the cathode. This is due to the high production term of metastable atoms by argon ion and atom impact excitations close to the cathode,[5] where the argon ions and atoms can reach high energies.[3] Farther away from the cathode, the argon metastable atom density decreases gradually. Indeed, the production of argon metastable atoms, caused by electron impact excitation in this region, is efficiently compensated by loss processes (primarily electron quenching to the nearby energy levels[5]). It reaches, however, a second, less pronounced maximum at about 9 mm from the cathode, since the loss processes are not important enough anymore to compensate to the same extent for the production of metastables. Away from the cell axis, the argon metastable atom density spreads out by diffusion and decreases gradually toward zero at the walls. The argon metastable number density is of the same order of magnitude as the argon ion number density[3] for our discharge conditions. This calculated argon metastable atom density profile, characterized by two peaks, is in reasonable qualitative agreement with the experimentally obtained profiles of refs 22 and 23. It is difficult to compare the absolute values with the results of ref 22, since these measurements were performed in a Grimm-type glow discharge, which operates at much higher pressures and currents. However, the results of the present model, when applied to a six-way cross glow discharge, are in satisfactory quantitative agreement with the experimental results obtained for the same discharge cell,[23] which is a validation of the present model.

In Figure 3, the argon metastable atom number densities at the maxima of their profiles are presented as a function of voltage at three pressures. The argon metastable atom number density clearly increases with voltage and pressure, as expected from the literature. However, it is found in the literature that, at sufficiently high-pressures, the argon metastable number density reaches a maximum, whereafter it decreases again, since the loss processes become more important than the production processes.[24-26] According to our calculations, such a pressure has not yet been reached. It was also not reached in the experiments of ref 23 (i.e., pressure range of 0.7−1.6 Torr).

The most important Ar^*_m production processes are fast argon ion and atom impact excitations close to the cathode and electron impact excitation at the beginning of the NG. Integrated over the complete three-dimensional geometry, these three processes account for about 17%, 70%, and 13%, respectively. The fact that argon ion and especially the argon atom impact excitations are so significant was not realized up to now. The cross sections of these processes are not so well described in the literature. The values that we adopted for these processes have to be considered

(21) Clark, J.; Greb, U.; Ronan, G.; Wheeler, D. Lecture presented at the 2nd International Conference on Plasma Source Mass Spectrometry, Durham, UK, 1990.

(22) Ferreira, N. P.; Strauss, J. A.; Human, H. G. C. *Spectrochim. Acta Part B* **1982**, *37*, 273−279.

(23) Bogaerts, A.; Guenard, R. D.; Smith, B. W.; Winefordner, J. D.; Harrison, W. W.; Gijbels, R. *Spectrochim. Acta Part B* submitted.

(24) Smith, R. L.; Serxner, D.; Hess. K. R. *Anal. Chem.* **1989**, *61*, 1103−1108.

(25) Browne, P. G.; Dunn, M. H. *J. Phys. B.* **1973**, *6*, 1103−1117.

(26) Hardy, K. A.; Sheldon, J. W. *J. Appl. Phys.* **1982**, *53*, 8532−8536.

as an upper limit.[27] When it is assumed that the mechanisms of electron impact excitation to the metastable level and argon ion and atom impact excitation to the metastable level are similar, it would be expected that their cross sections would also be of equal magnitude. Therefore, we have lowered the cross sections of argon ion and atom impact excitations to the metastable level by a factor of 2, so that the maxima are equal to the maximum in the cross section of electron impact excitation to the metastable level. Although it may still be that their contributions are somewhat overestimated, it seems that argon ion and atom impact excitations are quite important in determining the argon metastable atom number density at the high discharge voltages under consideration. The relative order of importance of these three production processes is maintained at all discharge conditions investigated; nevertheless, the relative contribution of electron impact excitation rises slightly with increasing pressure and decreasing voltage, since the argon ions and atoms then cannot reach such high energies and will cause reduced excitation. Electron–ion recombination can be considered negligible as production process of Ar^*_m at all discharge conditions investigated (i.e always <0.02%).

Diffusion toward regions of lower density, together with deexcitation at the walls, is mainly responsible for the loss of metastable atoms (i.e., about 82% over the total discharge volume). Besides diffusion, electron quenching is also a significant loss process, especially in the NG, where the slow electron number density is high;[3] integrated over the discharge region, electron quenching contributes about 11%. Penning ionization and metastable atom–metastable atom collisions also account for a small part of the total loss (about 3.7% and 3.0%, respectively) and are most significant close to the cathode, where the sputtered copper atom number density (see below) and the metastable atom number density are at their maximum. The remaining processes can be considered negligible for these discharge conditions (i.e., electron impact excitation and ionization from the metastable levels contribute to about 0.3% and 0.02%, respectively, and two-body and three-body collisions with argon atoms amount to about 0.1% and 0.01%, respectively). The relative role of the different loss processes is not influenced much by the discharge conditions. Diffusion seems always to be the dominant loss mechanism, and it becomes even more important at lower pressures and lower voltages. Electron quenching becomes a little more significant at lower voltages and higher pressures. The losses due to Penning ionization and metastable atom–metastable atom collisions increase slightly with pressure and voltage. The remaining four processes remain of minor significance at all discharge conditions investigated.

B. Results of the Sputtered Copper Atoms and Copper Ions. Figure 4 shows the thermalization profile of the sputtered copper atoms, i.e., the number of atoms thermalized per cubic centimeter at a given position (normalized to one sputtered atom). It is seen that the majority of the sputtered atoms are being thermalized very close to the cathode. Relatively few sputtered atoms can reach the anode backplate before being thermalized. This thermalization profile is used as a starting distribution to calculate the diffusion of the atoms.

The number density profile of the thermalized copper atoms at 75 Pa and 1000 V is presented in Figure 5. The copper atom number density reaches a maximum of about 6.7×10^{12} in front

(27) Phelps, A. V. *J. Phys. Chem. Ref. Data* **1991**, *20*, 557–573.

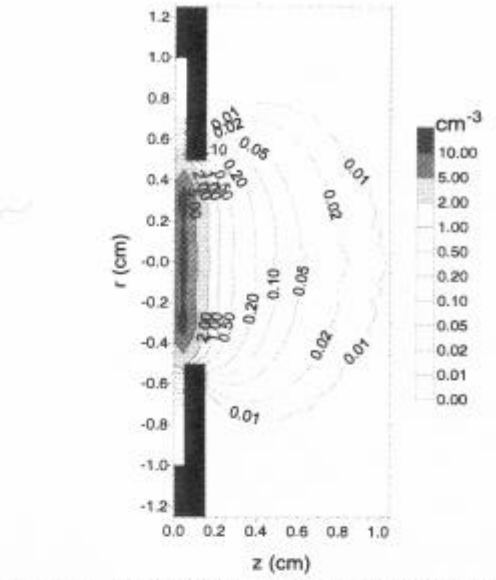

Figure 4. Thermalization profile of the sputtered copper atoms at 75 Pa and 1000 V.

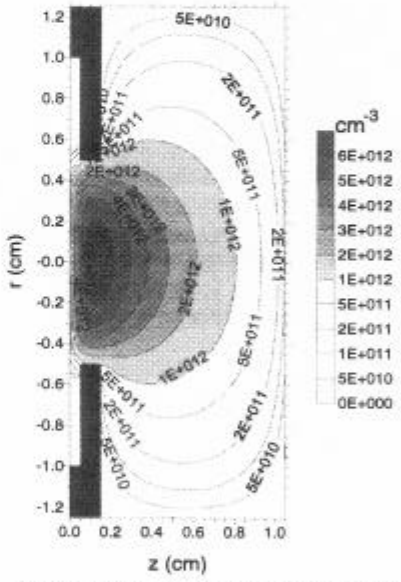

Figure 5. Density profile of the thermalized copper atoms at 75 Pa and 1000 V.

of the cathode and decreases gradually further in the discharge, towards low values at the cell walls. This is the result of the imposed boundary condition (i.e., $A_0 = 0.5$). At the end of this section, the effect of the sticking coefficient, A_0, will be briefly discussed. Besides the thermalized copper atoms, the nonthermalized atoms also contribute to the overall copper atom number density; their number density profile at 75 Pa and 1000 V is illustrated in Figure 6. Since Figure 4 showed that the sputtered atoms are already thermalized at a few millimeters from the cathode, most of the nonthermalized atoms can be found near the cathode. Therefore, the number density is at its maximum close to the cathode. It is seen that the nonthermalized atom density is negligible compared to the thermalized atom density,

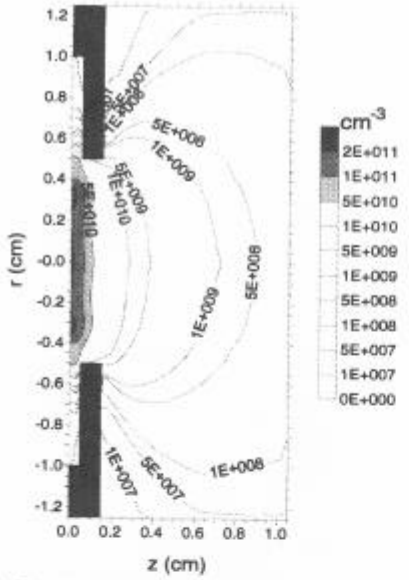

Figure 6. Density profile of the nonthermalized copper atoms at 75 Pa and 1000 V.

so that the thermalized copper atom number density and the overall copper atom number density profiles practically coincide.

The calculated copper atom number density profile, with a maximum at a few millimeters from the cathode, is in good qualitative agreement with number density profiles obtained experimentally by atomic absorption and fluorescence.[19,28-30] The "dip" in front of the cathode was explained in refs 28–30 by assuming that not all the cathode material is sputtered as neutral atoms, but that a certain amount is released as clusters or excited state species, which are not detected by atomic absorption or fluorescence. This explanation sounds quite reasonable. However, this profile also results from the modeling calculations, without the need to assume that the sputtered species occur in the form of clusters. Indeed, it is known that the sputtered atoms leave the cathode with energies of several electronvolts, and that they lose these initial energies very rapidly by collisions with argon gas atoms, until they are thermalized. This gives rise to the thermalization profile of Figure 4, which shows a maximum at about 1 mm from the cathode. This thermalization profile serves as starting distribution for the diffusion away from and back to the cathode. This explains why the sputtered atom population is at maximum at a few millimeters from the cathode. Indeed, a model where such an initial thermalization step is not included (e.g. ref 29) cannot predict the dip in front of the cathode. The experimentally obtained absolute values of the sputtered atom number densities are of the order of $(1-5) \times 10^{13}$ cm^{-3} for a hollow cathode lamp[11,31] and for a Grimm-type glow discharge.[29] Both types of discharges operate at much higher currents, so higher sputtered atom number densities are, indeed, expected. The modeling results are in excellent quantitative agreement with experimentally obtained profiles when measured in the same cell geometry as the one for which the model is applied, as is demonstrated in ref 19.

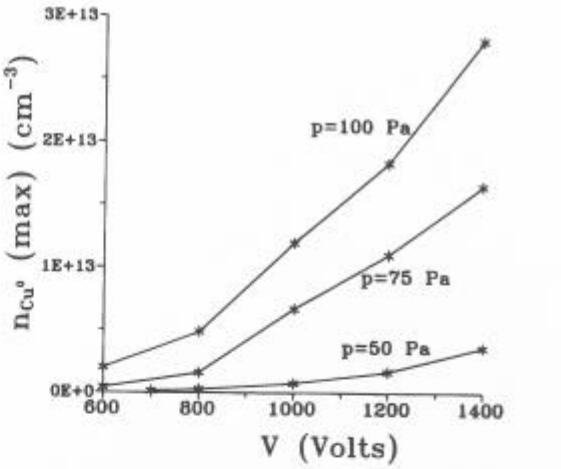

Figure 7. Maximum copper atom density as a function of voltage at three pressures.

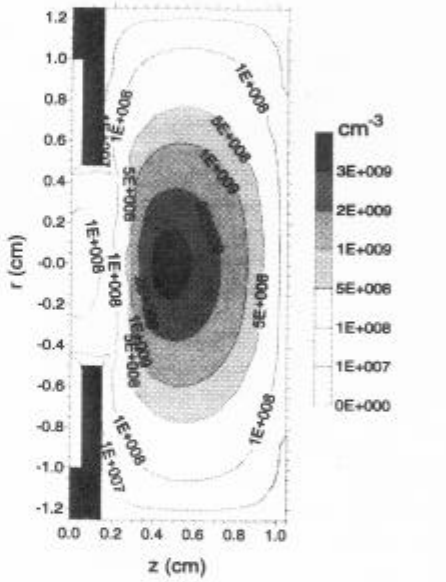

Figure 8. Density profile of the copper ions at 75 Pa and 1000 V.

Figure 7 illustrates the influence of pressure and voltage on the copper atom number density profile at its maximum. Higher pressures and voltages yield higher fluxes of ions and atoms bombarding the cathode; moreover, higher voltages result in higher energies of the bombarding particles, which gives more sputtering. Therefore, the sputtered copper atom number density increases with voltage and pressure.

Figure 8 shows the number density profile of the copper ions formed from the copper atoms, at 75 Pa and 1000 V. The number density is nearly constant in the CDS (~10^8 cm^{-3} or slightly less), increases rapidly in the NG, reaches a maximum of about 3.4×10^9 cm^{-3} at the center of the discharge, and decreases again to low values at the cell walls. This number density profile is also in reasonable agreement with the experimentally obtained number density profile, presented in ref 19. In Figure 9, the influence of voltage and pressure on the maximum value of the copper ion

(28) Stirling, A. J.; Westwood, W. D. *J. Phys. D: Appl. Phys.* **1971**, *4*, 246–252.
(29) Ferreira, N. P.; Human, H. G. C. *Spectrochim. Acta Part B* **1981**, *36*, 215–229.
(30) Hoppstock, K.; Harrison, W. W. *Anal. Chem.* **1995**, *67*, 3167–3171.
(31) de Hoog, F. J.; McNeil, J. R.; Collins, G. J.; Persson, K. B. *J. Appl. Phys.* **1977**, *48*, 3701–3704.

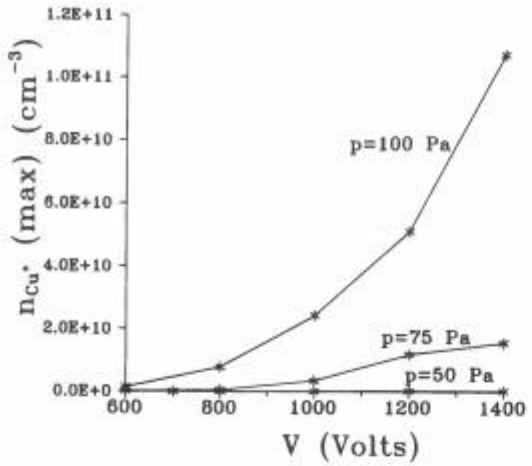

Figure 9. Maximum copper ion density as a function of voltage at three pressures.

number density is illustrated. The copper ion number density increases both with voltage and with pressure. The influence is clearly higher than that for the copper atoms. Indeed, the formation of copper ions depends on the copper atom number density and on the amount of ionization (i.e., by Penning ionization, asymmetric charge transfer, and electron impact ionization), and since both factors increase with pressure and voltage, the copper ion number density will increase more rapidly.

Figure 10, parts a–c, presents the ionization rates of copper atoms by Penning ionizaton, asymmetric charge transfer, and electron impact ionization, respectively. Penning ionization (Figure 10a) is most significant close to the cathode, where the argon metastable atom density is at its maximum (see before). Asymmetric charge transfer (Figure 10b) is especially important in the center of the NG, where the argon ion density reaches its maximum.[3] Electron impact ionization (Figure 10c) occurs mostly in the beginning of the NG, in analogy to electron impact ionization of argon atoms.[3] By comparison of the numerical values of the three ionization rates (i.e., Penning ionization shows a maximum of about 1.6×10^{15} cm^{-3} s^{-1}; the maximum of asymmetric charge transfer amounts to about 3.3×10^{14} cm^{-3} s^{-1}; and electron impact ionization reaches a maximum of about $6-7 \times 10^{13}$ cm^{-3} s^{-1}), it can be concluded that Penning ionization is the dominant ionization mechanism at these discharge conditions. Integrated over the total three-dimensional geometry, the relative contributions of Penning ionization, asymmetric charge transfer, and electron impact ionization to ionization of copper atoms amount to about 59%, 37%, and 4%, respectively. The relative contribution of electron impact ionization is somewhat higher than that calculated in the one-dimensional model.[5] Indeed, in the three-dimensional model, the number densities of the argon ions and argon metastable atoms are lower than those in the one-dimensional case, due to the wall effects. Hence, ionization of copper atoms by Penning ionization and asymmetric charge transfer will occur to a somewhat smaller degree, whereas electron impact ionization does not suffer from this effect. Therefore, the latter mechanism for ionizing copper atoms becomes somewhat less marginal in the three-dimensional model.

The contribution of asymmetric charge transfer to the ionization of copper is calculated to be almost as high as the role of Penning ionization at the present discharge conditions. Although in earlier reviews of GDMS, it has often been stated that Penning ionization is the dominant process and that asymmetric charge transfer only plays a secondary role, some other papers demonstrate that asymmetric charge transfer is very important in a glow discharge for certain ion–atom combinations.[15,32–38] Moreover, we have recently developed a model in which it was demonstrated that asymmetric charge transfer can explain the differences in relative sensitivity factors among different elements in GDMS.[39]

The relative contributions of these three ionization processes change slightly with pressure and voltage. Penning ionization seems clearly more dominant at low pressures (i.e., about 90% at 50 Pa, about 60% at 75 Pa, and about 35–40% at 100 Pa), whereas the reverse was found for asymmetric charge transfer (i.e., about 7–8% at 50 Pa, about 30–40% at 75 Pa, and about 50–60% at 100 Pa). Moreover, the relative importance of Penning ionization increases slightly, and that of asymmetric charge transfer decreases slightly at lower voltages. Electron impact ionization was always calculated to be of the order of 2–5%, slightly increasing with pressure, but nearly independent of voltage. These voltage and pressure effects are in qualitative agreement with experiment, since it is stated[40] that Penning ionization is dominant in low-pressure, low-current discharges and that asymmetric charge transfer becomes increasingly important in high-pressure, high-current glow discharges.

Comparing Figures 5 and 8, or Figures 7 and 9, gives us information about the ionization degree of copper. It is found that this ionization degree is of the order of 0.01–0.4%, and increases with voltage and pressure. These values are definitely lower than the results that we obtained in the one-dimensional approximation (i.e., about 1%[6]). Indeed, as mentioned above, Penning ionization and asymmetric charge transfer become less significant in the three-dimensional case, whereas electron impact ionization remains the same, and this results in a lower ionization degree. In the literature, "typical values" for the ionization degree of about 1% or less are usually mentioned,[1] which is higher than our present results. It is, however, not very clear where these values come from and hence how reliable they are. The discrepancy can, however, also indicate that our calculated results are not yet completely correct, although reasonable agreement with experiment has been recently found (see refs 19 and 23).

When we compare the calculated ionization degree of copper with the one of argon which is only of the order of 10^{-6}–10^{-5} (i.e., n_{Ar^+} and n_{Ar^0} are of the order of 10^{10}–10^{11} and 10^{16} cm^{-3}, respectively[3]), we can conclude that copper is still much more efficiently ionized than argon, due to Penning ionization and asymmetric charge transfer.

The copper ion number density profile (Figure 8) has the same shape as the argon ion number density profile[3] but is about 2 orders of magnitude lower. The copper ion-to-argon ion density ratio and the copper ion-to-argon ion flux ratio are, indeed, found

(32) Johansson, S.; Litzen, U. *J. Phys. B* **1978**, *11*, L703–L706.
(33) Danzmann, K.; Koch, M. *J. Phys. B* **1981**, *14*, 2989–2993.
(34) Farnsworth, P. B.; Walters, J. P. *Spectrochim. Acta Part B* **1982**, *37*, 773–788.
(35) Hudson, R. S.; Skrumeda, L. L.; Whaling, W. *J. Quant. Spectrosc. Radiat. Transfer* **1987**, *38*, 1–4.
(36) Steers, E. B. M.; Leis, F. *Spectrochim. Acta Part B* **1991**, *46*, 527–537.
(37) Steers, E. B. M.; Thorne, A. P. *J. Anal. At. Spectrom.* **1993**, *8*, 309–315.
(38) Wagatsuma, K.; Hirokawa, K. *Spectrochim. Acta Part B* **1996**, *51*, 349.
(39) Bogaerts, A.; Gijbels, R. *J. Anal. At. Spectrom.*, in press.
(40) Levy, M. K.; Serxner, D.; Angstadt, A. D.; Smith, R. L.; Hess. K. R. *Spectrochim. Acta, Part B* **1991**, *46*, 253–267.

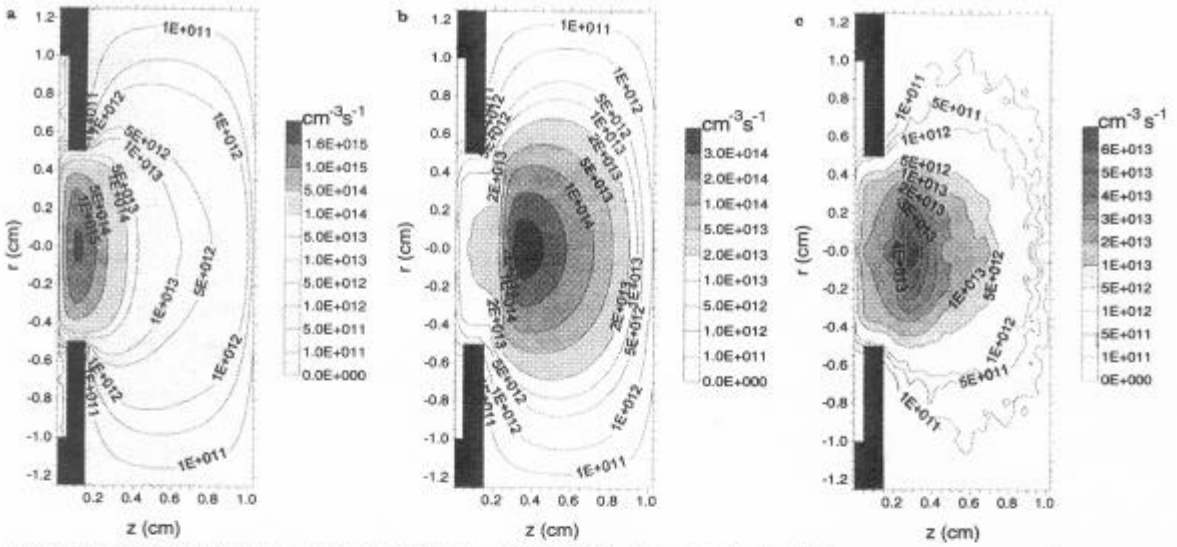

Figure 10. Ionization rate of the copper atoms at 75 Pa and 1000 V (a) by Penning ionization, (b) by asymmetric charge transfer, and (c) by electron impact ionization.

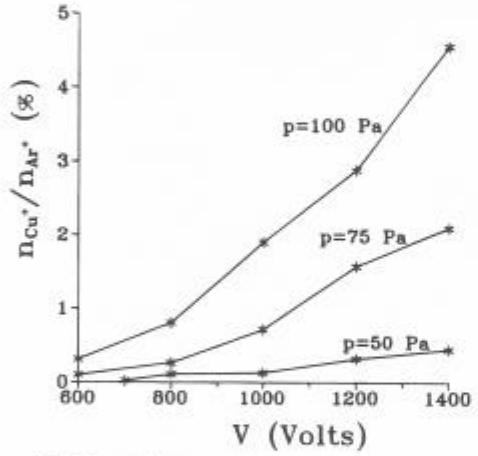

Figure 11. Copper ion-to-argon ion density ratio as a function of voltage at three pressures.

to be of the order of 1% at these discharge conditions. This is in reasonable agreement with experimental measurements of the ratio of copper ion peak to argon ion peak in the VG9000 mass spectrometer. Figure 11 shows that the calculated copper ion number density-to-argon ion number density ratio is in the order of 0.1−5%, and that it clearly increases with voltage and with pressure. It seems, therefore, advisable to work at high voltages and pressures, since this will give a better analytical sensitivity. However, in the VG9000 spectrometer, the voltage should not exceed 1.5 kV to avoid short-circuiting, and the pressure increase is limited by the coupling with the low-pressure mass spectrometer.

Just as in ref 6, we also calculated with the three-dimensional model the relative contribution of self-sputtering. The results were in complete agreement with those of the one-dimensional case. Indeed, the sputtering is caused mainly by fast argon atoms (i.e., about 60−70%), and the argon ions also have a large contribution (i.e., about 25−30%). However, the contribution of the copper ions (i.e., self-sputtering) is certainly not negligible, since these ions can reach the cathode with rather high energies.[6] They account for about 0.1−5%, and they become more significant at higher voltages and pressures.

As already mentioned, the sticking coefficient A_0 in the model was taken to be 0.5, because it yields the best agreement with experiment.[19] Since this value is actually unknown, we have performed the calculations with different values of A_0, ranging from 1 (100% sticking) to 0 (no sticking), to investigate its influence on the results. It was found that changing A_0 from 1 to 0 had a considerable effect. Indeed, the copper atom number density increased by more than 2 orders of magnitude, because the "sink" at the walls drops off gradually. Moreover, the pronounced maximum in the number density profile at a few millimeters from the cathode disappears. The effect of A_0 is, however, not linear; i.e., changing A_0 from 1 to 0.5 had a negligible influence on the shape and magnitude of the density profile, whereas the major effect is found for A_0 values close to zero (when A_0 is lowered from 0.001 to 0, an increase in density of almost a factor of 10 was found). Changing A_0 from 1 to 0 also yielded an increase in the copper ion density of 2 orders of magnitude. Also, the ratio of copper ion-to-argon ion flux and number density, and the contribution of copper ions to sputtering (self-sputtering) increased significantly (i.e., from about 1% at $A_0 = 1$ to about 50% at $A_0 = 0$). The effect is, however, always most significant at A_0 values close to zero and almost negligible at A_0 values ranging from 1 to 0.1. It is expected that the sticking coefficient is closer to 1 than to 0 (i.e., the majority of atoms will stick at the walls), and so using the value of 0.5 seems to be justified.

CONCLUSION

A two-dimensional model is developed to describe the behavior of argon metastable atoms and of copper atoms and ions in a dc glow discharge in argon. Typical results include the number densities of different species, the relative importance of different

production and loss processes of the argon metastable atoms, the thermalization profile of the sputtered copper atoms, the relative contributions of ionization mechanisms for the copper atoms, the ionization degree of copper, the copper ion-to-argon ion density ratio, and the relative roles of argon ions and fast atoms and of copper ions in the sputtering process. The effect of voltage and pressure on all these parameters is studied. Moreover, the influence of the sticking coefficient of copper atoms, which is not well-known in the literature, is briefly discussed. The reasonable agreement with experimental results[19,23] tells us that the model presents a realistic picture of the glow discharge and that it is quite useful to arrive at a better understanding of the glow discharge processes.

ACKNOWLEDGMENT

A.B. is indebted to the Belgian National Fund for Scientific Research (NFWO). The authors also acknowledge financial support from the Federal Services for Scientific, Technical and Cultural Affairs (DWTC/SSTC) of the Prime Minister's Office through IUAP-III (Conv. 49). We thank B. Smith and J. Winefordner for their help during the redaction of the manuscript.

Received for review December 13, 1995. Accepted May 10, 1996.*

AC951206Z

* Abstract published in *Advance ACS Abstracts*, June 15, 1996.